Kinetics of Granule Growth in Fluidized Bed Granulation with Moisture Control

Satoru WATANO,* Takashi MORIKAWA, and Kei MIYANAMI

Department of Chemical Engineering, University of Osaka Prefecture, 1–1 Gakuen-cho, Sakai, Osaka 593, Japan.
Received April 6, 1995; accepted June 30, 1995

The kinetics of granule growth in fluidized bed granulation with moisture control was theoretically investigated. A population balance equation, in which moisture content was taken into consideration for the coalescence probability of two colliding granules, was proposed. The effects of damping speed and operation time on granule growth during moisture fixed command control were numerically examined. It was found that an increase in operation time resulted in an enlargement of granule diameter and a narrow size distribution during the damping process, but no significant growth was observed in the moisture fixed command control process. By contrast, a decrease in the operation time (large damping speed) caused small granule growth in the damping process, but a large growth in the moisture control process. The theory also showed good agreement with experimental granulation data for pharmaceutical powders.

Key words population balance; kinetics; granulation; fluidized bed; moisture control

Moisture control has been widely used to control granule growth in fluidized bed granulation. This method has attracted considerable attention, especially in the pharmaceutical industries, because it can be a countermeasure for GMP (Good Manufacturing Practice) or process validation.

Up to this time, research related to the control of fluidized bed granulation has been directed mainly to the development of a moisture sensor or control system. One of the first attempts toward the moisture measurement was conducted by Hyland and Nauper,[1] who developed a moisture sensor using a water-sensitive polymer and then attempted to measure product moisture content. Shibata[2] and Nishii[3] developed an IR moisture sensor to continuously measure moisture content during granulation without touching the powder bed. Watano[4–6] developed a novel system for controlling moisture content during granulation. Although several studies[7] have already reported on granule growth during moisture control, there has been no theoretical approach to elucidate the growth mechanism. To control this process accurately, analysis of the binding mechanism and the kinetics of granule growth is required.

As for the binding mechanism, Rumpf[8] and Newitt and Conway-Jones[9] considered that granule growth by direct coalescence took place under appropriate moisture content, and that tumbling action kneaded a pair into a nearly spherical shape. In reference to this coalescence mechanism, Capes and Danckwertz,[10] Kapur *et al.*[11–13] and Ouchiyama and Tanaka[14–17] proposed various mathematical models. All of these models, however, lacked consideration of the fundamentals of pre-wetted powder granulation. In practice, the existence of granule surface water during a collision is necessary to form a liquid bridge, which produces an adhesion force between the colliding granules, leading to granule growth. On the other hand, Haung and Kono[18,19] refined the model by Ouchiyama and Tanaka[14–17] to express a coalescence probability function and a non-dimensional model predicting granule growth rate, in which the liquid bridge formation by colliding granules was taken into consideration. However, the correlation between the simulated and experimental data of granulation was not sufficient, and the effects of operating variables on granule growth were not fully investigated.

The purpose of the present study is to theoretically investigate the kinetics of granule growth in fluidized bed granulation. A population balance equation, in which moisture content is taken into consideration for coalescence probability, is proposed. The effects of damping speed and operation time on granule growth during a moisture fixed command control period (moisture content is maintained at a predetermined value constant) are numerically examined. To confirm the model's validity, the simulated results are compared with the experimental granulation data for standard pharmaceutical formulation.

Modeling of Granulation

Granule growth during granulation takes place by the effective coalescence between particles. To express granule growth by a population balance equation, the following assumptions have been used.

(i) Particles in the granulator are completely mixed and coalescence occurs by the combination of two spherical particles.

(ii) Coalescence occurs whenever adhesion force experiences to a pair.

(iii) Difficulty of coalescence is determined by a coalescence probability.

(iv) Attrition or crushing of granules is disregarded.

Assuming that a contact number function in completely mixed packing can be denoted as $n(D, d)$, the coalescence probability between particles of diameter D and d can be described as $P(D, d)$, and the loading frequency, which expresses the frequency of adhesion force (load) experienced to a pair, can be given as q, the number of pairs combined by the adhesion force between the particles of size fraction D—$D+\delta D$, and those of size fraction d—$d+\delta d$ at time t can be expressed as

* To whom correspondence should be addressed.

$$n(D,d)\delta D\delta d \times q \times P(D,d) = C'qN(t)C(D,d)P(D,d)f(D,t)f(d,t)\delta D\delta d = R(D,d)\delta D\delta d \quad (1)$$

where $N(t)$, $f(D,t)$ and $R(D,d)$ denote the total number of granules in a granulator at time t, frequency size distribution by number at time t, and a coalescence rate function. Also, C' and $C(D,d)$, which are defined as the packing parameter and number of contacts between the particles of diameter D and d, can be expressed as (see Appendix)

$$C' = 16(1-\varepsilon_A) \quad (2)$$

$$C(D,d) = \left(\frac{D+\bar{D}}{2\bar{D}}\right)^2\left(\frac{d+\bar{D}}{2\bar{D}}\right)^2 \Big/ \frac{3+\bar{D}^2/(\bar{D})^2}{4} \quad (3)$$

where ε_A is the surface porosity and $\bar{D}$ is an average diameter defined as follows:

$$\bar{D}^m = \int_0^\infty D^m f(D)\mathrm{d}D \quad \text{for } m=1,2 \quad (4)$$

According to the paper by Ouchiyama and Tanaka,[14-17] the number of particles going out of a specified size fraction D—$D+\Delta D$ in a unit time can be given as

$$N_{out} = \int_{d=0}^{\infty} R(D,d)\mathrm{d}d \times \Delta D\Delta t \quad (5)$$

and the number of granules coming into the size fraction in a unit time as

$$N_{in} = \frac{1}{2}\int_{d=0}^{D} R(\sqrt[3]{D^3-d^3}, d)\left(\frac{D}{\sqrt[3]{D^3-d^3}}\right)^2 \mathrm{d}d \times \Delta D\Delta t \quad (6)$$

Disregarding the granule crushing and attrition, $N_{in}-N_{out}$ should be equivalent to the number of accumulation between the size fraction of D—$D+\Delta D$. This relationship can be written as

$$\frac{\partial}{\partial t}[N(t)f(D,t)\Delta D] \times \mathrm{d}t = N_{in} - N_{out} \quad (7)$$

Substituting $R(D,d)$ into Eq. 7, and rearranging both sides of the above equation, the following expression is obtained.

$$\frac{\partial}{\partial t}[N(t)f(D,t)] = -C'qN(t)\int_0^\infty C(D,d)P(D,d)f(D,t)f(d,t)\mathrm{d}d + \frac{1}{2}C'qN(t)\int_0^D C(\sqrt[3]{D^3-d^3}, d)P(\sqrt[3]{D^3-d^3}, d) \times \left(\frac{D}{\sqrt[3]{D^3-d^3}}\right)^2 f(\sqrt[3]{D^3-d^3}, t)f(d,t)\mathrm{d}d \quad (8)$$

This equation expresses the basic population balance in a batch granulation system.

To make Eq. 8 dimensionless, the following equations are introduced.

$$u = D/\delta \quad (9)$$

$$v = d/\delta \quad (10)$$

where δ is a characteristic limiting size, which is defined as

$$P(D,d) = 0 \quad \text{at } D=d=\delta \quad (11)$$

Using Eqs. 9 and 10, Eq. 3 can be easily rewritten as

$$C(D,d) = C(u,v) = \left(\frac{u+\delta\bar{u}}{2\delta\bar{u}}\right)^2\left(\frac{v+\delta\bar{u}}{2\delta\bar{u}}\right)^2 \Big/ \frac{3+\bar{u}^2/\delta(\bar{u})^2}{4} \quad (12)$$

Thus, Eq. 8 is given as

$$\frac{\partial}{\partial t}[N(t)f(u,t)] = -C'q\delta N(t)\int_0^\infty C(u,v)P(u,v)f(u,t)f(v,t)\mathrm{d}v + \frac{1}{2}C'q\delta N(t)\int_0^u C(\sqrt[3]{u^3-v^3}, v)P(\sqrt[3]{u^3-v^3}, v) \times \left(\frac{u}{\sqrt[3]{u^3-v^3}}\right)^2 f(\sqrt[3]{u^3-v^3}, t)f(v,t)\mathrm{d}v \quad (13)$$

If we use dimensionless time τ, which expresses the frequency of adhesion force (load) per time t

$$\tau = c'qt \quad (14)$$

Eq. 13 can be rewritten as

$$\frac{\partial}{\partial \tau}[N(\tau)f(u,\tau)] = -\delta N(\tau)\int_0^\infty C(u,v)P(u,v)f(v,\tau)f(u,\tau)\mathrm{d}v + \frac{1}{2}\delta N(\tau)\int_0^u C(\sqrt[3]{u^3-v^3}, v)P(\sqrt[3]{u^3-v^3}, v) \times \left(\frac{u}{\sqrt[3]{u^3-v^3}}\right)^2 f(\sqrt[3]{u^3-v^3}, \tau)f(v,\tau)\mathrm{d}v \quad (15)$$

Multiplying $\delta\mathrm{d}u$ on both sides of the above equation, and integrating it between $u=0$—∞, the left side of Eq. 15 becomes

$$\text{(left side)} = \delta\int_0^\infty \frac{\partial}{\partial\tau}[N(\tau)f(u,\tau)]\mathrm{d}u = \delta\int_0^\infty\left[\frac{\partial N(\tau)}{\partial\tau}\cdot f(u,\tau) + \frac{\partial f(u,\tau)}{\partial\tau}\cdot N(\tau)\right]\mathrm{d}u = \frac{\partial N(\tau)}{\partial\tau}\delta\int_0^\infty f(u,\tau)\mathrm{d}u + N(\tau)\delta\int_0^\infty\frac{\partial f(u,\tau)}{\partial\tau}\mathrm{d}u \quad (16)$$

Substituting

$$\delta\int_0^\infty f(u,\tau)\mathrm{d}u = 1 \quad (17)$$

and,

$$\int_0^\infty \frac{\partial f(u,\tau)}{\partial\tau}\mathrm{d}u = 0 \quad (18)$$

which express that the sum of the frequency distribution per unit time is zero, the left side of Eq. 15 can be described as

$$\delta\int_0^\infty\frac{\partial}{\partial\tau}[N(\tau)f(\delta u,\tau)]\mathrm{d}u = \frac{\partial}{\partial\tau}N(\tau) \quad (19)$$

Similarly, the right side of Eq. 15 is given as

$$\text{(right side)} = -\delta^2N(\tau)\int_0^\infty\int_0^\infty C(u,v)P(u,v)f(u,\tau)f(v,\tau)\mathrm{d}v\mathrm{d}u + \frac{1}{2}\delta^2N(\tau)\int_0^\infty\int_0^u\left[C(\sqrt[3]{u^3-v^3}, v)P(\sqrt[3]{u^3-v^3}, v) \times \left(\frac{u}{\sqrt[3]{u^3-v^3}}\right)^2 f(\sqrt[3]{u^3-v^3}, \tau)f(v,\tau)\right]\mathrm{d}v\mathrm{d}u \quad (20)$$

Therefore, the dimensionless change rate of the number of granules can be given by the combination of Eqs. 19 and 20.

$$\frac{\partial}{\partial\tau}N(\tau)=-\delta^2N(\tau)\int_0^\infty\int_0^\infty C(u,v)P(u,v)f(u,\tau)f(v,\tau)\mathrm{d}v\mathrm{d}u+\frac{1}{2}\delta^2N(\tau)\int_0^\infty\int_0^u\left[C(\sqrt[3]{u^3-v^3},v)P(\sqrt[3]{u^3-v^3},v)\times\left(\frac{u}{\sqrt[3]{u^3-v^3}}\right)^2f(\sqrt[3]{u^3-v^3},\tau)f(v,\tau)\right]\mathrm{d}v\mathrm{d}u \quad (21)$$

Furthermore, substituting Eq. 21 into Eq. 15, and dividing it by $N(\tau)$, the following expression is obtained.

$$\begin{aligned}\frac{\partial}{\partial\tau}f(u,\tau)=&-\delta\int_0^\infty C(u,v)P(u,v)f(v,\tau)f(u,\tau)\mathrm{d}v\\&+\frac{1}{2}\delta\int_0^u\left[C(\sqrt[3]{u^3-v^3},v)P(\sqrt[3]{u^3-v^3},v)\times\left(\frac{u}{\sqrt[3]{u^3-v^3}}\right)^2f(\sqrt[3]{u^3-v^3},\tau)f(v,\tau)\right]\mathrm{d}v\\&+\delta^2\int_0^\infty\int_0^\infty C(u,v)P(u,v)f(u,\tau)f(v,\tau)\mathrm{d}v\mathrm{d}u\\&-\frac{1}{2}\delta^2\int_0^\infty\int_0^u\left[C(\sqrt[3]{u^3-v^3},v)P(\sqrt[3]{u^3-v^3},v)\times\left(\frac{u}{\sqrt[3]{u^3-v^3}}\right)^2f(\sqrt[3]{u^3-v^3},\tau)f(v,\tau)\right]\mathrm{d}v\mathrm{d}u\end{aligned} \quad (22)$$

Since frequency distribution after infinitely small time can be expressed as

$$f(u,\tau+\Delta\tau)=f(u,\tau)+\frac{\partial f(u,\tau)}{\partial\tau}\Delta\tau \quad (23)$$

the frequency distribution of granules after $\Delta\tau$ can be calculated by means of Eq. 23.

In this simulation, whether two particles adhered or not in collision has been judged by a coalescence probability, then the change in frequency distribution has been calculated using Eq. 22. By integrating the change in the frequency distribution using Eq. 23, the frequency distribution of particles can be calculated with passage of time.

Difficulty of coalescence between particles is determined by a coalescence probability. In this study, a dimensionless coalescence probability introduced by Ouchiyama and Tanaka[14-17] has been basically used.

$$P(D,d)=P(u,v)=\lambda^n\left[1-\left\{\frac{(uv)^{\gamma-3\eta/2}}{\left(\frac{u+v}{2}\right)^{2\gamma-4-3\eta/2}}\right\}^{2/(3\zeta)}\right]^n \quad (24)$$

where η and ζ are physical constants dependent on the physical properties of a powder; according to Herts,[20] $\zeta=1$ and $\eta=0$ was equivalent to plastic, and $\zeta=\eta=2/3$ was to elastic. In addition, Kapur and Fuerstenau[13] have reported that the granule growth rate of batch granulation increases with the increasing moisture content of granules. This facts implies that the coalescence probability between the two contacting granules increases with increasing moisture content. Thus, the parameters of coalescence probability (Eq. 24) must be determined in relation to moisture content dependence.

Experimental

Equipment A schematic diagram of an experimental apparatus is illustrated in Fig.1. For wet granulation, an agitation fluidized bed[4-7,21] (NQ-125, Fuji Paudal Co., Ltd.) with a vessel diameter of 125 mm was used. In this fluidized bed, an agitator blade was equipped to create tumbling and compacting effects on granules, making the granules spherical and well-compacted. Under the blade, three circular plates of different diameters were superimposed 3 mm apart to function as an air distributor. Heated air for particle fluidization was blown from the slits between each circular plate to create a circulating flow. Fine powders lifted up by the fluidization air were entrapped by bag filters and brushed down by a pulsating jet of air.

The moisture content of granules during granulation was measured by an infrared (IR) moisture sensor (Wet-eye, Fuji Paudal Co., Ltd.).[5-7] Based on the preliminary correlation between the IR absorbance and moisture content measured by a drying method, moisture content by a wet basis was measured automatically.

Powder Samples Table 1 gives the properties of powder samples used. The starting materials for granulation were a pharmaceutical formulation, which consisted of lactose and cornstarch (mixed at 7:3 by weight). Hydroxypropylcellulose was added to the above mixture at a level of 5 wt% before granulation. Purified water was sprayed by a binary nozzle located at the top of the vessel (the top spray method).

Figure 2 shows the size distribution of particles used for both simulation and actual granulation. In this figure, plots show the size distribution of particles used for actual granulation, and a line indicates the size distribution of particles used for the simulation. Particles used for actual granulation obeyed log-normal distribution and had a 33 μm number median diameter and a 1.55 geometric standard deviation. The particle size distribution used for simulation was calculated to be the same particle size distribution as the powder samples used for actual granulation experiments.

Operating Conditions Basic operating conditions for the granulation experiments are summarized in Table 2.

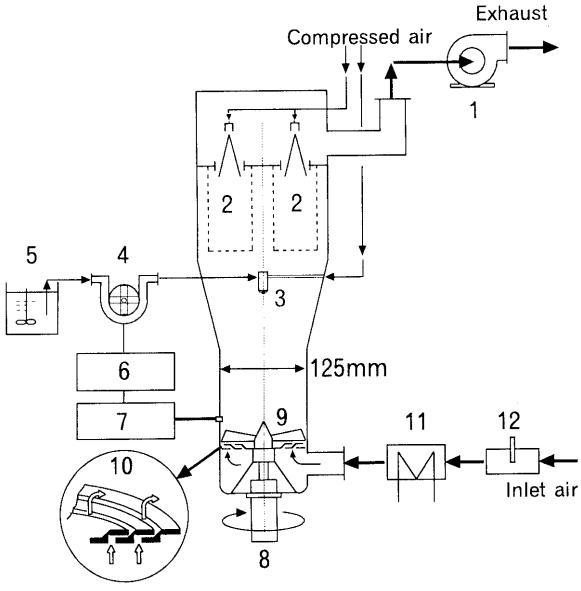

Fig. 1. Schematic Diagram of Experimental Apparatus Employed

1, blower; 2, bag filter; 3, spray nozzle; 4, pump; 5, binder liquid; 6, controller; 7, IR moisture sensor; 8, motor; 9, agitator blade; 10, slit plate; 11, heater; 12, hot-wire anemometer.

Table 1. List of Powder Samples Used

Sample	Number median diameter (μm)	Mixing weight (kg)
Lactose[a]	60	0.21
Cornstarch[b]	15	0.09
Hydroxypropylcellulose[c]	21	0.015
Total		0.315

a) Pharmatose 200 M, DMV. *b*) Corn starch W, Nippon Shokuhin Kakou Co., Ltd. *c*) HPC-EFP, Shin-Etsu Chemical Co., Ltd.

Granulation experiments were conducted as follows.

(i) Premixed powder samples were fed to the vessel and agitated with fluidization air for 300 s.

(ii) Granulation experiments started with spraying water. As shown in Fig. 3, the moisture content was programmed to increase with predetermined damping speed. Here, dW/dt shows a damping speed which is equivalent to the percent increase in moisture content per unit minute (for example, $dW/dt=1.0$ shows that the moisture content is increased by 1% per 1 min). In this contribution, heated air temperature has been regulated to control the damping speed. This method was intended to keep a constant spray mist size.

(iii) After reaching 15%, the moisture content was maintained at 15% for 10 min by a moisture fixed command control. At this point, we tried to investigate granule growth during this moisture fixed command control region by both theoretical and experimental approaches.

Evaluation of Granulated Products Number-based particle size distributions of granulated products and powder samples were measured using an image processing system[21] (Image Eye, Fuji Paudal Co., Ltd.).

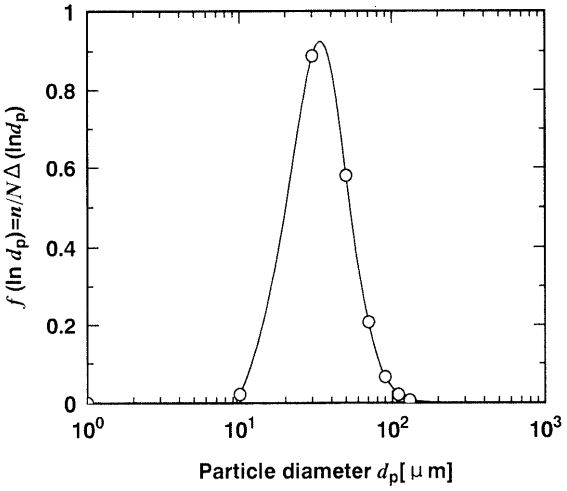

Fig. 2. Size Distribution of Particles Used for Simulation
○, actual granulation; —, simulation.

Table 2. Operating Conditions

Inlet air velocity	0.6 m/s
Inlet air temperature	333 K
Agitator rotational speed	5.0 rps
Average spray mist size	40 μm
Spray nozzle height	100 mm
Nozzle insert	1.0 mm (i.d.)
Spray air pressure	1.5×10^5 Pa

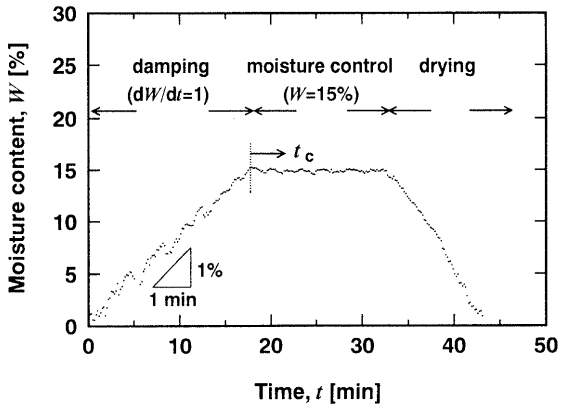

Fig. 3. Example of Moisture Control

Results and Discussion

Determination of Coalescence Probability When we applied a population balance equation for analysis of the granule growth process, determination of coalescence probability was the most important.

First, parameters η and ζ in Eq. 24 were determined. According to Ouchyama and Tanaka,[15] η and ζ were physical constants dependent on the physical properties of powder. They stated that $\zeta=1$ and $\eta=0$ was equivalent to plastic, and $\zeta=\eta=2/3$ was equivalent to elastic. They also examined the moisture content dependence of coalescence probability; however, there was no concrete data for these parameters and moisture content dependence.

In this study, we determined these parameters as follows: granulation using the pharmaceutical powder (Table 1) can be conducted when the moisture content W is between 0 and 20%. If the moisture content is greater than 20%, the granule-water packing condition is nearly slurry, leading to blocking or defluidization. Thus, we assumed that the granules at $W=0\%$ were equivalent to plastic ($\zeta=1$, $\eta=0$), and granules at $W=20\%$ were equivalent to elastic ($\zeta=\eta=2/3$); in addition, the parameters of ζ and η varied in proportion to the moisture content. Thus, the parameters can be given as

$$\eta=-\frac{1}{30}W+\frac{2}{3} \tag{25}$$

$$\zeta=\frac{1}{60}W+\frac{2}{3} \tag{26}$$

Based on the above relation, the parameters during the constant moisture control maintaining $W=15\%$ were determined to be $\eta=0.1667$ and $\zeta=0.9167$.

Secondly, we have determined parameters n and γ. It has been reported that the granule growth rate of batch granulation increases with the increasing moisture content of granules.[13] This facts implies that the coalescence probability between two contacting granules increases with an increasing moisture content.[10] However, in the moisture control granulation, it could be assumed that the adhesion force was constant; parameters n and γ were also suggested to be independent of moisture content.

Figures 4 and 5 show granule number median diameter and geometric standard deviation at various n. Here, lines and plots indicate simulated and experimental data, respectively. Also, t_c was an elapsed time from the beginning of the moisture fixed command control as described in Fig. 3. With a decrease in n, granule growth was promoted, leading to a large granule size and narrow size distribution. In case of the $n=3$, the simulated results agreed well with the experimental data. Therefore, we have determined that the optimum n was 3.

As to the parameter γ, γ should be greater than $(3/2)\eta$, because $P(D, d)>0$ was applicable under the region of $\gamma>(3/2)\eta$. Thus we determined that γ could be expressed as a form of $\gamma>(3/2)\eta+\alpha$; we varied constant α to determine the optimum value.

Figures 6 and 7 describe the effect of α on granule number median diameter and geometric standard deviation. With an increase in α, the median diameter and the deviation were prone to increase. In the case of $\alpha=3$, the

simulated results agreed well with the experimental data. Thus, the parameter α was determined to be 3.

According to the paper by Ouchiyama and Tanaka,[15] a model parameter of λ was defined by

$$\lambda=\frac{Q_M}{Q_M-Q_m} \tag{27}$$

where, Q_M and Q_m showed the maximum and minimum compressive force between two granules. Assuming that the minimum compressive force is zero, the parameter of λ is determined to be 1. In this study, we have used $\lambda=1$ to express the coalescence probability.

Figure 8 illustrates coalescence probability at various colliding granule sizes. As seen in Fig. 8, the coalescence probability indicated that coalescence was easy if the colliding granule size was small under the same moisture content.

Analysis of Granule Growth during Moisture Control

Figures 9 and 10 indicate the effect of damping speed on the number median diameter and the geometric standard deviation of granules during the moisture control process.

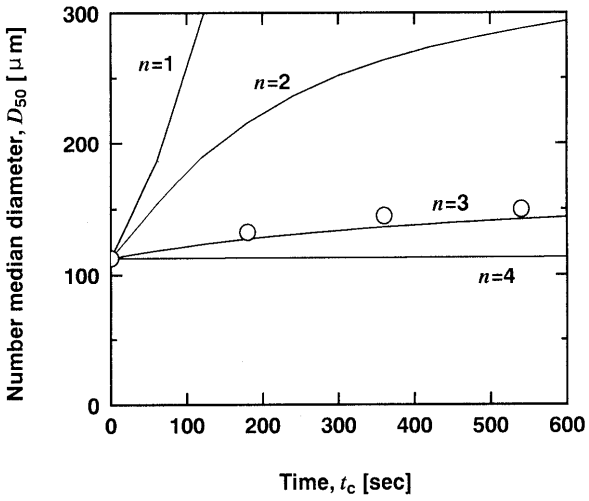

Fig. 4. Effect of Parameter n on Granule Number Median Diameter
○, experimental data; —, calculated data.

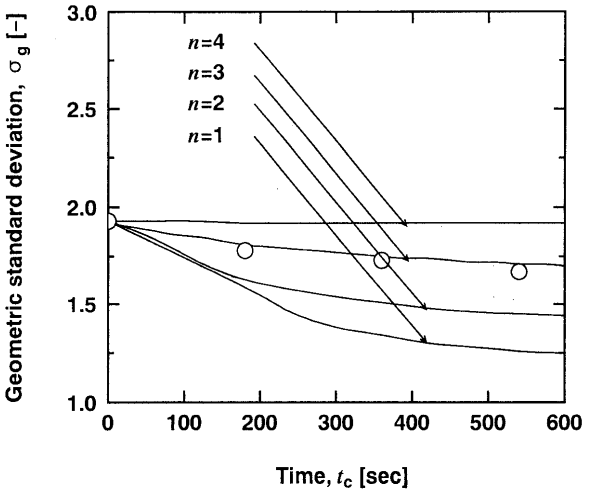

Fig. 5. Effect of Parameter n on Geometric Standard Deviation of Granules
○, experimental data; —, calculated data.

In this simulation, to express the effect of the damping speed during granulation, the model parameters related to the moisture content such as η and ζ in the coalescence

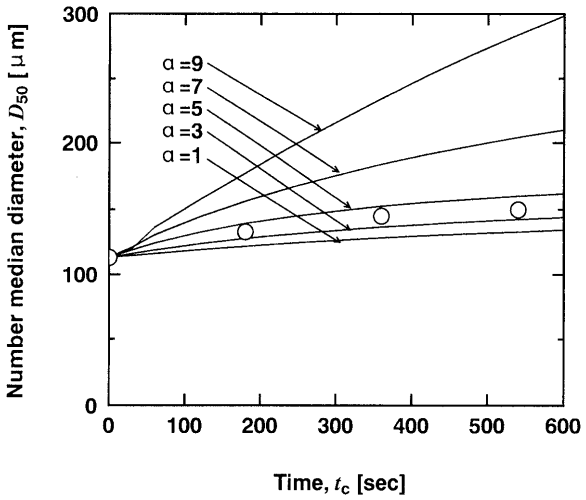

Fig. 6. Effect of Parameter α on Granule Number Median Diameter
○, experimental data; —, calculated data.

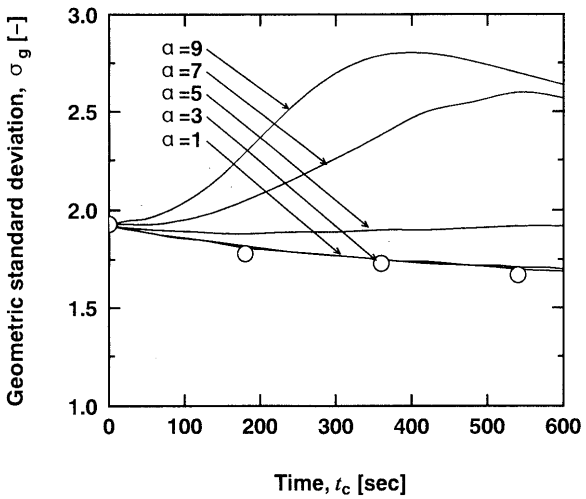

Fig. 7. Effect of Parameter α on Geometric Standard Deviation of Granules
○, experimental data; —, calculated data.

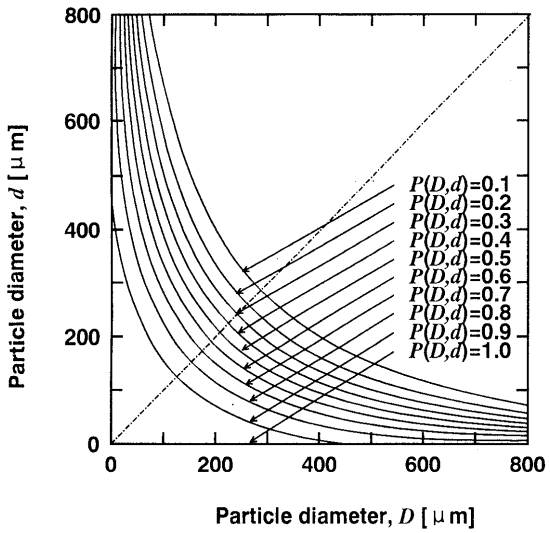

Fig. 8. Graphic Representation of Coalescence Probability ($W=15\%$)

probability have changed with a predetermined damping speed. Thus, granule growth as a function of both moisture content and granulation time can be calculated numerically. Here, the phenomenon that the diameter and the deviation at $t_c=0$ varied with the damping speed originated from the fact that the granule growth in the damping process was different due to the damping speed variation. In the moisture command control region, however, the coalescence probability was kept constant, because the adhesion force between the two colliding granules was maintained at a constant value due to the moisture control.

As seen in Figs. 9 and 10, it was found that granules in the moisture fixed command control region showed marked growth in the case of a large damping speed (dW/dt was large), while it indicated no significant growth in the case of a small damping speed.

To examine the granule growth mechanism more particularly, we investigated the change in frequency size distribution of granules at various damping speeds. Figures 11, 12 and 13 give the results obtained. In the case of a small damping speed (time required for the damping process was large), granule growth at the beginning of the moisture control ($t_c=0$) was sufficiently promoted because of the large operation time, *i.e.*, the great frequency with which the adhesion force could be received during the damping process caused the granule size to be large and the size distribution narrow. By contrast, in the case of the large damping speed, granules showed insufficient growth at the beginning of moisture control ($t_c=0$); granule size was small and its distribution was broad. With an increase in elapsed time, only a small fraction of granules were adhered, while the large fraction of granules were not altered much. This was because the enlargement of large granules was suppressed, since the coalescence probability was kept constant ($W=15\%$ constant). By contrast, the growth of small granules was promoted with the lapse of processing time. This difference in granule growth rate (*i.e.*, the smaller the granule size, the faster the growth rate), and the phenomena that the maximum granule size was kept constant, caused the size distribution to move to the right direction and become narrow.

The difference in growth rate due to a variation of damping speed could be also explained by the growth mechanism. For example, when the damping speed was large (time required for the damping process was small), the granules showed wide size distribution and had a large

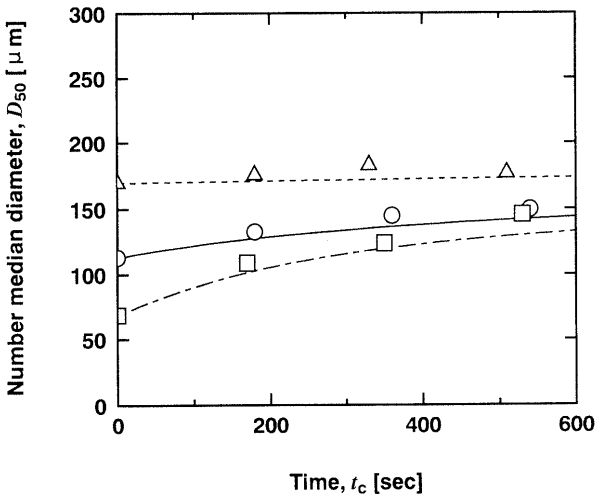

Fig. 9. Effect of Damping Speed on Number Median Diameter of Granules

Experimental data; △, $dW/dt=0.5$; ○, $dW/dt=1.0$; □, $dW/dt=2.0$. Calculated data; – – –, $dW/dt=0.5$; ——, $dW/dt=1.0$; —·—, $dW/dt=2.0$.

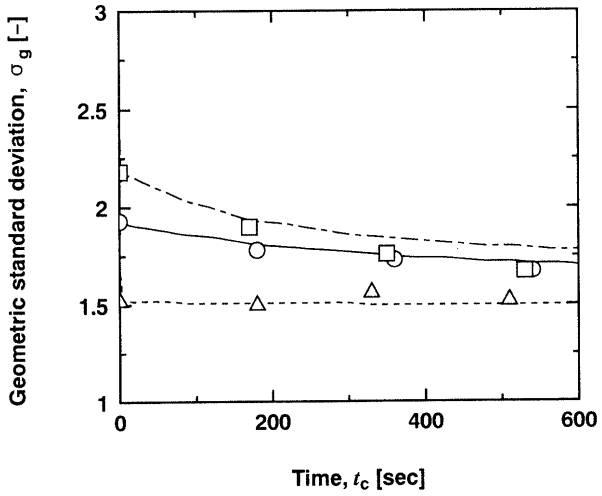

Fig. 10. Effect of Damping Speed on Geometric Standard Deviation of Granules

Experimental data; △, $dW/dt=0.5$; ○, $dW/dt=1.0$; □, $dW/dt=2.0$. Calculated data; – – –, $dW/dt=0.5$; ——, $dW/dt=1.0$; —·—, $dW/dt=2.0$.

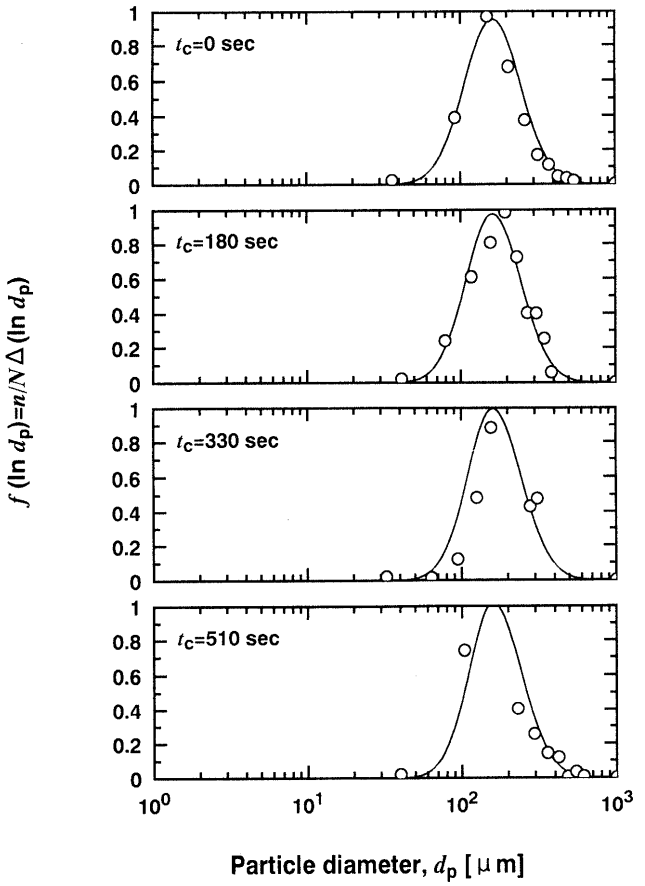

Fig. 11. Change in Particle Size Distribution during Moisture Control Process ($dW/dt=0.5$)

○, experimental data; —, calculated data.

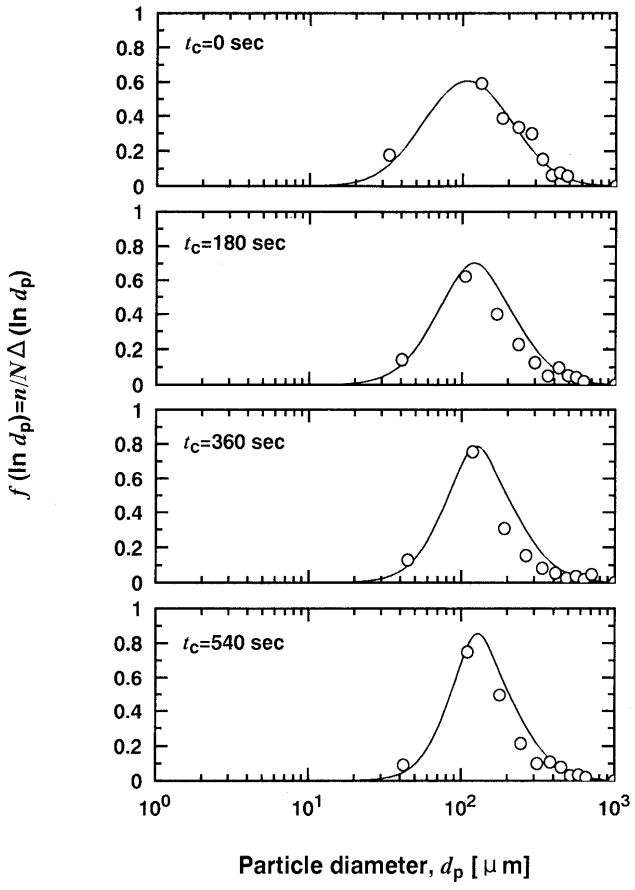

Fig. 12. Change in Particle Size Distribution during Moisture Control Process ($dW/dt=1.0$)

○, experimental data; —, calculated data.

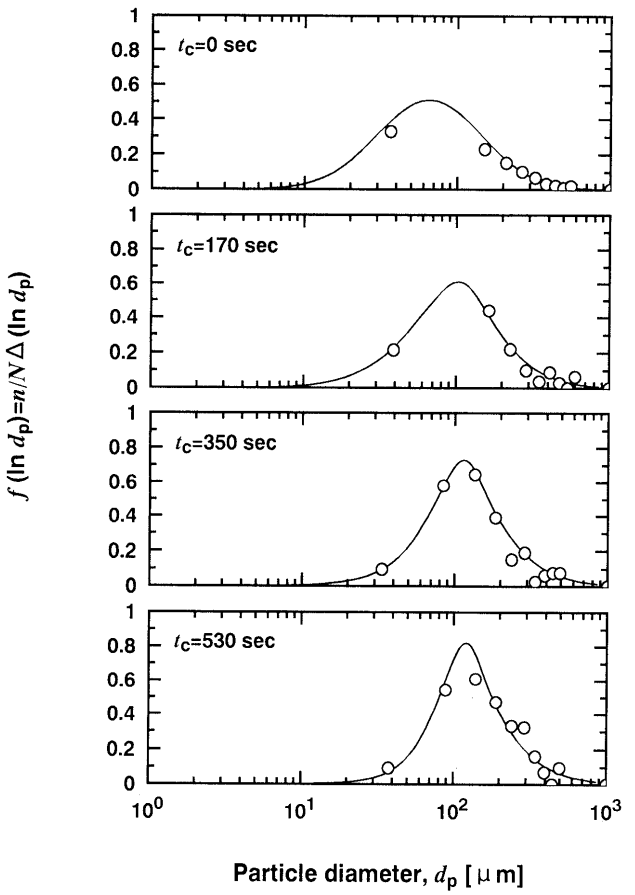

Fig.13 Change in Particle Size Distribution during Moisture Control Process ($dW/dt=2.0$)

○, experimental data; —, calculated data.

amount of small fraction. In this case, the change in size distribution during the moisture fixed command control region was rapid because the granule growth of a small fraction was promoted despite the constant adhesion force. By contrast, in case of the small damping speed (large processing time), granule growth was hardly observed because the granules of the small fraction were already enlarged during the damping process. Therefore, marked growth was found in case of large damping speed (dW/dt was large), while no significant growth was indicated in the case of the small damping speed.

As a result, the granule growth mechanism was elucidated and the effects of damping speed on granule growth were analyzed theoretically by means of the simulation model proposed here. In addition, extremely good correlation was obtained between the simulated and experimental data of granulation, which implied that the coalescence probability in the population balance equation expressed the granulation phenomena correctly.

Conclusion

A population balance equation, in which moisture content was taken into consideration for the coalescence probability of two colliding granules, was proposed to investigate the kinetics of granule growth in fluidized bed granulation under moisture control. The effects of damping speed and operation time on granule number median diameter and geometric standard deviation were numerically examined. As a result, the granule growth mechanism within a moisture control region was elucidated theoretically. The difference in granule growth behavior at various damping speeds could also be explained by a proposed model. It was again found that the simulated results were in good agreement with experimental granulation data for pharmaceutical powders.

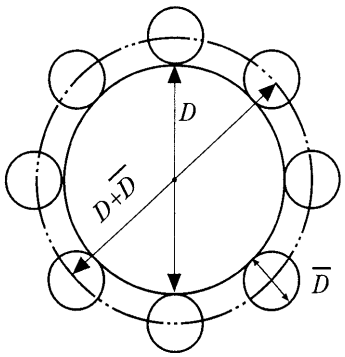

Fig. 14. Random Packing Model

Appendix

Model for Random Packing Figure 14 illustrates a basic random packing model for the theoretical analysis of contact number. Let us assume that spherical particles of diameter $\bar{D}$ are randomly placed on a solid sphere of diameter D. The number of contacts $C(D)$ between the spherical particles on the solid sphere was discussed by Ouchiyama and Tanaka[16] as,

$$C(D)=\frac{\text{(substantial surface area of } D+\bar{D})}{\text{(projected area of particle } \bar{D})}$$
$$=\frac{4\pi(1-\varepsilon_A)\left(\frac{D+\bar{D}}{2}\right)^2}{\pi\left(\frac{\bar{D}}{2}\right)^2}=16(1-\varepsilon_A)\left(\frac{D+\bar{D}}{2\bar{D}}\right)^2 \quad (28)$$

where ε_A shows surface porosity.

Number of Contacts between the Particles Assuming that the total number of particles is N, particles of size fraction x—$x+\mathrm{d}x$ have contacting points $C(d)Nf(d)\mathrm{d}d$. Therefore, the total number of contacting points in a bed, C_T, can be expressed as

$$C_T=\int_0^\infty C(d)Nf(d)\mathrm{d}d$$
$$=\int_0^\infty 16(1-\varepsilon_A)\left(\frac{d+\bar{d}}{2\bar{d}}\right)^2 Nf(d)\mathrm{d}d$$
$$=16(1-\varepsilon_A)\cdot N\cdot\frac{1}{4(\bar{d})^2}$$
$$\cdot\left\{\int_0^\infty d^2f(d)\mathrm{d}d+2\bar{d}\int_0^\infty df(d)\mathrm{d}d+(\bar{d})^2\int_0^\infty f(d)\mathrm{d}d\right\}$$
$$=16(1-\varepsilon_A)N\cdot\frac{3+\bar{d}^2/(\bar{d})^2}{4} \quad (29)$$

Here, Eq. 4 was used to arrange the above Eq. 29. The probability that a contacting point should make a pair with a contacting point of particles d—$d+\mathrm{d}\delta$ can be described as $C(d)Nf(d)\delta d/C_T$. The number of pairs between particles of the size fraction of D—$D+\delta D$ and those of size fraction d—$d+\delta d$ can be expressed as

$$n(D,d)\delta D\delta d=16(1-\varepsilon_A)\frac{\left(\frac{D+\bar{D}}{2\bar{D}}\right)^2\left(\frac{d+\bar{D}}{2\bar{D}}\right)^2}{\frac{3+\bar{d}^2/(\bar{d})^2}{4}}Nf(D)f(d)\delta D\delta d$$
$$=C'\cdot C(D,d)Nf(D)f(d)\delta D\delta d \quad (30)$$

If we introduce the concept of coalescence probability and time into the above equation, Eq. 1 can be easily obtained.

References

1) Hyland M., Naunapper D., *Drugs Made in Germany*, **31**, 29—36 (1988).
2) Shibata T., *Funtai Kougaku Kaishi*, **24**, 374—378 (1987).
3) Nishii K., Proc. of the 7th Symposium on Particulate Preparations and Designs, *Funtai Kougaku Kaishi*, pp. 94—96 (1989).
4) Watano S., Terashita K., Miyanami K., *Bull. Univ. Osaka Pref.*, **39**, 187—197 (1990).
5) Watano S., Sato Y., Miyanami K., *J. Chem. Eng. Jpn.*, **28**, 282—287 (1995).
6) Watano S., Fukushima T., Miyanami K., *Powder Technol.*, **81**, 161—168 (1994).
7) Watano S., Yamamoto A., Miyanami K., *Chem. Pharm. Bull.*, **42**, 133—137 (1994).
8) Rumpf H., *Chemie. Ingr. Tech.*, **30**, 144—158 (1958).
9) Newitt D. M., Conway-Jones J. M., *Trans. Inst. Chem. Eng.*, **22**, 422—441 (1958).
10) Capes C. E., Danckwertz P. V., *Trans. Inst. Chem. Eng.*, **43**, 125—130 (1965).
11) Kapur P. C., Fuerstenau D. W., *Trans. Am. Inst. Min., Metal., Pet. Engrs.*, **229**, 348—353 (1964).
12) Kapur P. C., Fuerstenau D. W., *Ind. Eng. Chem. Process Des. Develop.*, **5**, 5—14 (1966).
13) Kapur P. C., Fuerstenau D. W., *Ind. Eng. Chem. Process Des. Develop.*, **8**, 56—62 (1969).
14) Ouchiyama N., Tanaka T., *Ind. Eng. Chem. Process Des. Develop.*, **13**, 383—389 (1974)
15) Ouchiyama N., Tanaka T., *Ind. Eng. Chem. Process Des. Develop.*, **14**, 286—289 (1975).
16) Ouchiyama N., Tanaka T., *Ind. Eng. Chem. Process Des. Develop.*, **20**, 340—348 (1981).
17) Ouchiyama N., Tanaka T., *Ind. Eng. Chem. Process Des. Develop.*, **21**, 29—35 (1982).
18) Hang C. C., Kono H., *Powder Technol.*, **55**, 19—34 (1988).
19) Hang C. C., Kono H., *Powder Technol.*, **55**, 35—49 (1988).
20) Timoshenko S., Goodier J. N., "Theory of Elasticity," 3rd ed., Mcgrew Hill, New York, 1970, p. 409.
21) Watano S., Miyanami K., *Powder Technol.*, **83**, 55—60 (1994).